THERMO-FLUIDIC PARAMETERS EFFECTS ON NONLINEAR VIBRATION OF FLUID-CONVEYING NANOTUBE RESTING ON ELASTIC FOUNDATIONS USING HOMOTOPY PERTURBATION METHOD

M. G. Sobamowo[1,*], A. A. Yinusa[1]

ABSTRACT

In this paper, effects of thermo-fluidic parameters on the nonlinear dynamic behaviours of single-walled carbon nanotube conveying fluid with slip boundary conditions and resting on linear and nonlinear elastic foundations under external applied tension and global pressure is studied using homotopy perturbation method. From the result, it is observed that increase in the Knudsen number, the slip parameter, leads to decrease in the frequency of vibration and the critical velocity while natural frequency and the critical fluid velocity increase as the in stretching effect increases. Also, as the Knudsen number increases, the bending stiffness of the nanotube decreases and in consequent, the critical continuum flow velocity decreases as the curves shift to the lowest frequency zone. As the change in temperature increases, the natural frequencies and the critical flow velocity of the structure increase for the low or room temperature while at high temperature, increase in temperature change, decreases the natural frequencies and the critical flow velocity of the structure. Further, it is established that the alteration of nonlinear flow-induced frequency from linear frequency is significant as the amplitude, flow velocity and axial tension increase. The developed analytical solutions can be used as starting points for better understanding of the relationship between the physical quantities of the problem.

Keywords: Thermo-Fluidic Effects, Non-Linear Vibration, Slip Boundary Condition, Fluid-Conveying Nanotube, Homotopy Perturbation Method

INTRODUCTION

There have been increasing interests and rapid developments in the study of nanotube following the discovery of Iijima [1]. As part of the numerous applications, carbon nanotube (CNT) has been used for conveying/transporting fluid and the study of effects and the conditions of moving fluid on the overall mechanical behaviour of CNTs have been an area that has aroused significant and challenging research interests. Consequently, the dynamic analysis of flow-induced vibration of CNT has attracted a large number of studies in literatures in recent years [2-15]. Modeling the dynamic behaviours of the structures under the influence of some thermo-fluidic or thermo-mechanical parameters often results in nonlinear equations and such are difficult to find the exact analytical solutions. In some cases where decomposition procedures into spatial and temporal parts are carried out, the resulting nonlinear equation for the temporal part comes in form of Duffing equation (a second-order differential equation with cubic or quintic nonlinearity). Since, it is difficult to find an exact analytical solution for the nonlinear equation, approximate analytical solutions are sought for. In such an adventure, perturbation method has proven to be a well-known and most versatile method in nonlinear analysis of engineering problems, but its limitations hamper its applications [16]. It is a method based on existence of or assuming a small parameter and in solutions, in most cases, are valid only for small values of the small parameter [16-20]. However, an overwhelming majority of nonlinear problems, especially those having strong nonlinearity, have no small parameter at all [16-20]. Also, there is no criterion on which the small parameter should exist and the determination of small parameters seems to be a special art requiring special techniques. In order to overcome this difficulty, many different new methods have recently introduced such as Exp-function method, artificial parameter method, He's Exp-function method, δ-expansion method, improved F-expansion method, quotient trigonometric function expansion method, cubication method, quantification method, Newton's harmonic balancing method, variational iteration method, homotopy perturbation method, homotopy analysis method, Adomian decomposition method, differential transformation method [21-29] etc. However, the development of analytical solutions by most of these new methods often involved complex mathematical analysis leading to analytic expression involving a large number terms. In practice, analytical solutions with large number of terms and conditional statements for the solutions are not convenient for use by designers and engineers [30, 31]. Consequently, in many research works, recourse has been made to numerical methods in solving the problems. However, the classical way for finding analytical solution is obviously still very important since it serves as an accurate benchmark for numerical

solutions. When such analytical solutions are available, they provide good insights into the significance of various system parameters affecting the phenomena. Approximate analytical solutions such as homotopy analysis method (HAM) is a reliable and efficient semi-analytical technique, but it suffers from a number of limiting assumptions such as the requirements that the solution ought to conform to the so-called rule of solution expression and the rule of coefficient ergodicity. Also, the use of HAM in the analysis of linear and nonlinear equations requires the determination of auxiliary parameter which will increase the computational cost and time. Also, the lack of rigorous theories or proper guidance for choosing initial approximation, auxiliary linear operators, auxiliary functions, and auxiliary parameters limit the applications of HAM. Moreover, such method requires high skill in mathematical analysis and the solution comes with large number of terms. In practice, analytical solutions with large number of terms and conditional statements for the solutions are not convenient for use by designers and engineers [32].

The determination of Adomian polynomials as carried out in Adomian decomposition method (ADM), the need for small perturbation parameter as required in traditional PMs, the rigour of the derivations of differential transformations or recursive relation as carried out in differential transformation method (DTM), the lack of rigorous theories or proper guidance for choosing initial approximation, auxiliary linear operators, auxiliary functions, auxiliary parameters, and the requirements of conformity of the solution to the rule of coefficient ergodicity as done in HAM, the search Langrange multiplier as carried out in variational iteration method (VIM), and the challenges associated with proper construction of the approximating functions for arbitrary domains or geometry of interest as in Galerkin weighted residual method (GWRM), least square method (LSM) and collocation method (CM) are some of the difficulties that are not experienced in HPM. Furthermore, in the class of the newly developed approximate analytical methods, homotopy perturbation method is considered to relatively simple with fewer requirements for mathematical rigour or skill. HPM solves differential equations, difference equation, differential-difference equations, fractional differential equation, pantograph equation and integro-differential equation. It solves nonlinear integral and differential equations without linearization, discretization, closure, restrictive assumptions, perturbation, approximations, round-off error and discretization that could result in massive numerical computations. It does not require small parameter in the algebraic or differential equation as done in the other traditional perturbation methods (Regular and singular perturbation). It provides excellent approximations to the solution of non-linear equation with high accuracy. Also, most of the above methods are limited to small domains. Applying the methods to large or infinite domain problems are often carried out with the applications of before-treatment techniques such as domain transformation techniques, domain truncation techniques and conversion of the boundary value problems to initial value problems or with the use of after-treatment techniques such as Pade-approximant, basis function, cosine after-treatment techniques, sine-after-treatment techniques and domain decomposition techniques. Indisputably, such additional computations through the before- and after-treatment techniques increase the computational cost and time. Furthermore, the search for a particular value that will satisfy second the boundary condition in DTM, HAM, ADM, and VIM necessitated the use of software and such could result in additional computational cost in the generation of solution to the problem. This drawback in the other approximation analytical methods is not experienced in HPM. HPM is a powerful method that gives acceptable analytical and accurate results with convenient convergence and stability [16-20]. Therefore, in finding approximate analytical solutions to linear and nonlinear differential equations, HPM has fast gained ground as it appeared in many engineering and scientific research papers. Although, the improved HPM such as optimal homotopy asymptotic method (OHAM), optimal homotopy perturbation method (OHPM), homotopy analysis method (HAM), Optimal homotopy analysis method (OHAM) give higher accurate results than HPM but this comes with increased computational cost and time. In the class of the newly developed approximate analytical methods, homotopy perturbation method is considered to be relatively simple with fewer requirements for mathematical rigour or skill. Therefore, in this work, homotopy perturbation method is used to study the effects of thermo-fluidic parameters on the nonlinear dynamic behaviors of single-walled carbon nanotube conveying fluid with slip boundary conditions. Galerkin's decomposition procedure is employed to decompose the developed nonlinear partial differential equation of motion governing the nonlinear vibration of nanotube conveying fluid. Homotopy perturbation method is applied to develop approximate analytical solution for temporal part of the decomposed equation. Based on the verifications and validation carried out in this work, it could be stated that the analytical solutions as developed in this work can serve as a starting point for a better understanding of the relationship between the physical quantities of the problems.

Problem formulation based on nonlocal beam theory

Consider a single-walled carbon nanotube conveying hot fluid, subjected to stretching effects and resting on linear and nonlinear elastic foundations under external applied tension and global pressure as shown in Figure 1. Based on the Eringen's nonlocal elasticity theory [31-35] and Hamilton's principle, we arrived at the governing equation of motion for the single-walled carbon nanotube (SWCNT) as;
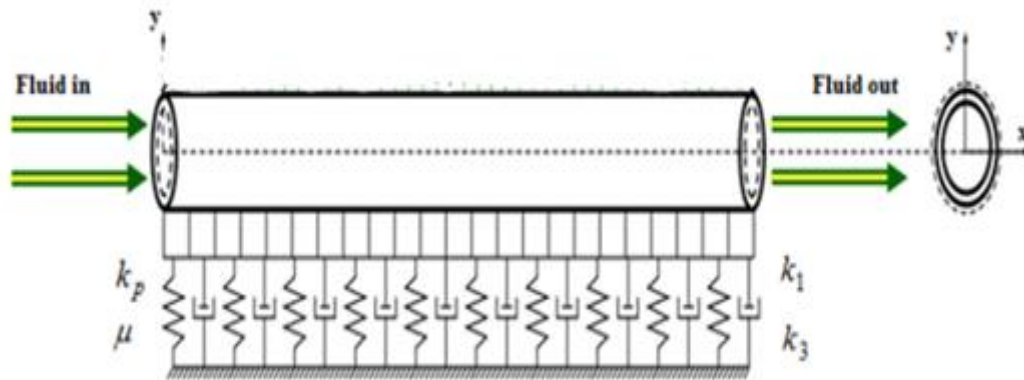
Figure 1. a fluid-conveying single-walled carbon nanotube (SWCNT) resting on elastic foundation

$$EI\frac{\partial^4 w}{\partial x^4}+(m_p+m_f)\frac{\partial^2 w}{\partial t^2}+\mu\frac{\partial w}{\partial t}+2vm_f\frac{\partial^2 w}{\partial x\partial t}+\left(m_f v^2+PA-T-k_p-\frac{EA\alpha\Delta\theta}{1-2v}\right)\frac{\partial^2 w}{\partial x^2}-\left[\frac{EA}{2L}\int_0^L\left(\frac{\partial w}{\partial x}\right)^2 dx\right]\frac{\partial^2 w}{\partial x^2}$$

$$+k_1 w+k_3 w^3-(e_o a)^2\left[\begin{array}{l}(m_p+m_f)\dfrac{\partial^4 w}{\partial x^2\partial t^2}+\mu\dfrac{\partial^3 w}{\partial x^2\partial t}+k_1\dfrac{\partial^2 w}{\partial x^2}+6k_3 w\left(\dfrac{\partial w}{\partial x}\right)^2+3w^2\dfrac{\partial w}{\partial x}+2vm_f\dfrac{\partial^4 w}{\partial x^3\partial t}\\[3mm]+\left(m_f v^2+PA-T-k_p-\dfrac{EA\alpha\Delta\theta}{1-2v}\right)\dfrac{\partial^4 w}{\partial x^4}-\left[\dfrac{EA}{2L}\int_0^L\left(\dfrac{\partial w}{\partial x}\right)^2 dx\right]\dfrac{\partial^4 w}{\partial x^4}\end{array}\right]=0$$

(1)

The derivation of the governing equation (although, with some modifications to include effects of elastic foundation, axial tension, global pressure and temperature change in this paper) has been shown in the author's previous paper [36].

If the nanotube is slightly curved, then the governing equation for the nanotube becomes

$$EI\frac{\partial^4 w}{\partial x^4}+(m_p+m_f)\frac{\partial^2 w}{\partial t^2}+\mu\frac{\partial w}{\partial t}+2vm_f\frac{\partial^2 w}{\partial x\partial t}+\left(m_f v^2+PA-T-k_p-\frac{EA\alpha\Delta\theta}{1-2v}\right)\frac{\partial^2 w}{\partial x^2}$$

$$-\left[N_o+\frac{EA}{2L}\int_0^L\left\{\frac{\partial Z_o}{\partial x}\frac{\partial w}{\partial x}+\left(\frac{\partial w}{\partial x}\right)^2\right\}dx\right]\left[\frac{\partial^2 w}{\partial x^2}+\frac{\partial^2 Z_o}{\partial x^2}\right]+k_1 w+k_3 w^3$$

$$-(e_o a)^2\left[\begin{array}{l}(m_p+m_f)\dfrac{\partial^4 w}{\partial x^2\partial t^2}+\mu\dfrac{\partial^3 w}{\partial x^2\partial t}+k_1\dfrac{\partial^2 w}{\partial x^2}+6k_3 w\left(\dfrac{\partial w}{\partial x}\right)^2+3w^2\dfrac{\partial w}{\partial x}+2vm_f\dfrac{\partial^4 w}{\partial x^3\partial t}\\[3mm]+\left(m_f v^2+PA-T-k_p-\dfrac{EA\alpha\Delta\theta}{1-2v}\right)\dfrac{\partial^4 w}{\partial x^4}-\left[N_o+\dfrac{EA}{2L}\int_0^L\left\{\dfrac{\partial Z_o}{\partial x}\dfrac{\partial w}{\partial x}+\left(\dfrac{\partial w}{\partial x}\right)^2\right\}dx\right]\left[\dfrac{\partial^4 w}{\partial x^4}+\dfrac{\partial^4 Z_o}{\partial x^4}\right]\end{array}\right]=0$$

(2)

Where $Z_o(x)$ is the arbitrary initial rise function.

For nanotube conveying fluid, the radius of the tube is assumed to be the characteristics length scale, Knudsen number is larger than 10^{-2}. Therefore, the assumption of no-slip boundary conditions does not hold and modified model should be used. Therefore, we have

$$VCF = \frac{U_{avg,slip}}{U_{avg,no-slip}} = \left(1 + a_k Kn\right)\left[4\left(\frac{2-\sigma_v}{\sigma_v}\right)\left(\frac{Kn}{1+Kn}\right)+1\right] \tag{3}$$

Where Kn is the Knudsen number, σ_v is tangential moment accommodation coefficient which is considered to be 0.7 for most practical purposes [37, 38].

$$a_k = a_o \frac{2}{\pi}\left[tan^{-1}\left(a_1 Kn^B\right)\right] \tag{4a}$$

$$a_o = \frac{64}{3\pi\left(1-\dfrac{4}{b}\right)} \tag{4b}$$

Therefore,

$$U_{avg,slip} = \left(1 + a_k Kn\right)\left[4\left(\frac{2-\sigma_v}{\sigma_v}\right)\left(\frac{Kn}{1+Kn}\right)+1\right]U_{avg,no-slip} = VCF\left(U_{avg,no-slip}\right) \tag{5}$$

And Equation (2) could be written as

$$EI\frac{\partial^4 w}{\partial x^4} + (m_p+m_f)\frac{\partial^2 w}{\partial t^2} + \mu\frac{\partial w}{\partial t} + 2m_f\left[VCF\left(U_{avg,no-slip}\right)\right]\frac{\partial^2 w}{\partial x \partial t} + \left(m_f\left[VCF\left(U_{avg,no-slip}\right)\right]^2 + PA - T - k_p - \frac{EA\alpha\Delta\theta}{1-2v}\right)\frac{\partial^2 w}{\partial x^2}$$

$$-\left[N_o + \frac{EA}{2L}\int_0^L\left\{\frac{\partial Z_o}{\partial x}\frac{\partial w}{\partial x} + \left(\frac{\partial w}{\partial x}\right)^2\right\}dx\right]\left[\frac{\partial^2 w}{\partial x^2} + \frac{\partial^2 Z_o}{\partial x^2}\right] + k_1 w + k_3 w^3$$

$$-\left(e_o a\right)^2\left[\begin{array}{l}(m_p+m_f)\dfrac{\partial^4 w}{\partial x^2 \partial t^2} + \mu\dfrac{\partial^3 w}{\partial x^2 \partial t} + k_1\dfrac{\partial^2 w}{\partial x^2} + 6k_3 w\left(\dfrac{\partial w}{\partial x}\right)^2 + 3w^2\dfrac{\partial w}{\partial x} + 2m_f\left[VCF\left(U_{avg,no-slip}\right)\right]\dfrac{\partial^4 w}{\partial x^3 \partial t}\\[3mm] +\left(m_f\left[VCF\left(U_{avg,no-slip}\right)\right]^2 + PA - T - k_p - \dfrac{EA\alpha\Delta\theta}{1-2v}\right)\dfrac{\partial^4 w}{\partial x^4} - \left[N_o + \dfrac{EA}{2L}\int_0^L\left\{\dfrac{\partial Z_o}{\partial x}\dfrac{\partial w}{\partial x} + \left(\dfrac{\partial w}{\partial x}\right)^2\right\}dx\right]\left[\dfrac{\partial^4 w}{\partial x^4} + \dfrac{\partial^4 Z_o}{\partial x^4}\right]\end{array}\right] = 0 \tag{6}$$

The initial and the boundary conditions

In this work, different boundary conditions are considered for the nanotube.

Clamped-Clamped (doubly clamped)

Where the trial/comparison function are given as;

$$\phi(x) = cosh\lambda_n x - cos\lambda_n x - \left(\frac{cosh\lambda_n L - cos\lambda_n L}{sinh\lambda_n L - sin\lambda_n L}\right)\left(sinh\lambda_n x - sin\lambda_n x\right) \tag{7a}$$

or

$$\phi(x) = \cosh\lambda_n x - \cos\lambda_n x - \left(\frac{\sinh\lambda_n L + \sin\lambda_n L}{\cosh\lambda_n L - \cos\lambda_n L}\right)\left(\sinh\lambda_n x - \sin\lambda_n x\right) \tag{7b}$$

where λ_n are the roots of the equation

$$\cos\lambda_n L \cosh\lambda_n L = 1$$

The initial and the boundary conditions are

$$w(x,0) = a, \ \dot{w}(x,0) = 0 \tag{8}$$

$$w(0,t) = w'(0,t) = 0, w(L,t) = w'(L,t) = 0 \tag{9}$$

The applications of space function as given above for clamped-clamped will involve long calculations and expressions in finding M, G, K, C, and V, alternatively, a polynomial function of the form Equation (10) can be applied for this type of support system.

$$\phi(x) = a_o + a_1 X + a_2 X^2 + a_3 X^3 + a_4 X^4 \tag{10}$$

where $X = \dfrac{x}{L}$

Applying the boundary conditions

$$\phi(x) = \left(X^2 - 2X^3 + X^4\right)a_4 \tag{11}$$

Orthogonal function should satisfy the equation

$$\int_0^a \phi(X)\phi(X)dx = 1 \tag{12}$$

Substitute Equation (11) into Equation (12), we have

$$a_4 = 3\sqrt{70}\left(\sqrt{\frac{1}{a^5\left(70a^4 - 315a^3 + 540a^2 - 420a + 126\right)}}\right) \tag{13}$$

For $a = 1$, arrived at $a_4 = 25.20$ for the first mode

Clamped-Simple supported
The trial/comparison function is given as

$$\phi(x) = \cosh\lambda_n x - \cos\lambda_n x - \left(\frac{\cosh\lambda_n L - \cos\lambda_n L}{\sinh\lambda_n L - \sin\lambda_n L}\right)\left(\sinh\lambda_n x - \sin\lambda_n x\right) \tag{14}$$

λ_n are the roots of the equation

$$tan\lambda_n L = tanh\lambda_n L$$

The initial and the boundary conditions are

$$w(x,0) = a, \dot{w}(x,0) = 0 \tag{15}$$

$$w(0,t) = w'(0,t) = 0, w(L,t) = w''(L,t) = 0 \tag{16}$$

Alternatively, a polynomial function of the form in Equation (17) can be applied for this type of support system.

$$\phi(x) = \left(\frac{3}{2}X^2 - \frac{5}{2}X^3 + X^4\right)a_4 \tag{17}$$

On using orthogonal functions, $a_4 = 11.625$ for the first mode

Simple-Simple supported

$$\phi(x) = sin\lambda_n x \tag{18}$$

$$sin\lambda_n L = 0 \quad \Rightarrow \lambda_n = \frac{n\pi}{L}$$

The initial and the boundary conditions are

$$w(x,0) = a, \dot{w}(x,0) = 0 \tag{19}$$

$$w(0,t) = w''(0,t) = 0, w(L,t) = w''(L,t) = 0 \tag{20}$$

Alternatively, a polynomial function of the form in Equation (21) can be applied for this type of support system.

$$\phi(x) = \left(X - 2X^3 + X^4\right)a_4 \tag{21}$$

On using orthogonal functions, $a_4 = 3.20$ for the first mode

Clamp-Free (cantilever)

$$\phi(x) = cosh\lambda_n x - cos\lambda_n x - \left(\frac{cosh\lambda_n L + cos\lambda_n L}{sinh\lambda_n L + sin\lambda_n L}\right)\left(sinh\lambda_n x - sin\lambda_n x\right) \tag{22}$$

or

$$\phi(x) = cosh\lambda_n x - cos\lambda_n x - \left(\frac{sinh\lambda_n L - sin\lambda_n L}{cosh\lambda_n L - cos\lambda_n L} \right) \left(sinh\lambda_n x - sin\lambda_n x \right) \qquad (23)$$

λ_n are the roots of the equation

$$cos\lambda_n L cosh\lambda_n L = -1$$

The initial and the boundary conditions are

$$w(x,0) = a, \dot{w}(0,x) = 0 \qquad (24)$$

$$w(0,t) = w'(0,t) = 0, w''(L,t) = w'''(L,t) = 0 \qquad (25)$$

Alternatively, a polynomial function of the form Equation (26) can be applied for this type of support system.

$$\phi(x) = \left(6X^2 - 4X^3 + X^4 \right) a_4 \qquad (26)$$

Also, with the aid of orthogonal functions, $a_4 = 0.6625$ for the first mode

The Spatial and Temporal Decomposition Procedures
Using the Galerkin's decomposition procedure to separate the spatial and temporal parts of the lateral displacement functions as

$$w(x,t) = \phi(x)u(t)$$

$$(27)$$

where $u(t)$ the generalized coordinate of the system and $\phi(x)$ is a trial/comparison function that will satisfy both the geometric and natural boundary conditions.

Applying one-parameter Galerkin's solution given in Equation (1) and Equation (2)

$$\int_0^L R(x,t)\phi(x)dx \qquad (28)$$

$$M\ddot{u}(t) + G\dot{u}(t) + (K+C)u(t) - Vu^3(t) = 0 \qquad (29)$$

where

$$M = \int_0^L (m_p + m_f)\phi(x) \left(\phi(x) - (e_o a)^2 \frac{d^2\phi}{dx^2} \right) + \phi(x) \left(m_f u^2 \phi(x) - (e_o a)^2 \frac{d^2\phi}{dx^2} \right) dx$$

$$G = \int_0^L \phi(x) \left\{ \left(2m_f v \frac{d\phi}{dx} - (e_o a)^2 \frac{d^3\phi}{dx^3} \right) + \left(\mu\phi(x) - (e_o a)^2 \frac{d^2\phi}{dx^2} \right) \right\} dx$$

$$K = \int_0^L \phi(x) \left\{ EI \frac{d^4\phi}{dx^4} + k_1\phi(x) - k_p \frac{d^2\phi}{dx^2} - k_1 (e_o a)^2 \frac{d^2\phi}{dx^2} + (e_o a)^2 k_p \frac{d^2\phi}{dx^2} \right\} dx$$

$$C = \int_0^L \left(m_f u^2 + PA - T - \frac{EA\alpha\Delta\theta}{1-2v} \right) \phi(x) \left(\frac{d^2\phi}{dx^2} - (e_o a)^2 \frac{d^4\phi}{dx^4} \right) dx$$

$$V = \int_0^L \phi(x) \left\{ \begin{array}{c} \left[N_o + \frac{EA}{2L} \int_0^L \left(\frac{\partial\phi}{\partial x} \right)^2 dx \right] \frac{d^2\phi}{dx^2} - k_3 \frac{d^3\phi}{dx^3}(x) + 6k_3(e_o a)^2 \phi(x) \left(\frac{\partial\phi}{\partial x} \right)^2 \\ -3k_3(e_o a)^2 \phi^2(x) \frac{\partial\phi}{\partial x} - (e_o a)^2 \left[N_o + \frac{EA}{2L} \int_0^L \left(\frac{\partial\phi}{\partial x} \right)^2 dx \right] \frac{d^4\phi}{dx^4} \end{array} \right\} dx$$

For the slightly curved nanotube, *M, G, K* and *C* are the same but

$$V = \int_0^L \phi(x) \left\{ \begin{array}{c} \left[N_o + \frac{EA}{2L} \int_0^L \left\{ \frac{\partial Z_o}{\partial x} \frac{\partial w}{\partial x} + \left(\frac{\partial w}{\partial x} \right)^2 \right\} dx \right] \left[\frac{\partial^2 w}{\partial x^2} + \frac{\partial^2 Z_o}{\partial x^2} \right] - k_3 \frac{d^3\phi}{dx^3}(x) + 6k_3(e_o a)^2 \phi(x) \left(\frac{\partial\phi}{\partial x} \right)^2 \\ -3k_3(e_o a)^2 \phi^2(x) \frac{\partial\phi}{\partial x} - (e_o a)^2 \left[N_o + \frac{EA}{2L} \int_0^L \left\{ \frac{\partial Z_o}{\partial x} \frac{\partial w}{\partial x} + \left(\frac{\partial w}{\partial x} \right)^2 \right\} dx \right] \left[\frac{\partial^4 w}{\partial x^4} + \frac{\partial^4 Z_o}{\partial x^4} \right] \end{array} \right\} dx$$

and the circular fundamental natural frequency gives

$$\omega_n = \sqrt{\frac{K + C^*}{M}} \tag{30}$$

where

$$C^* = \int_0^L \left(PA - T - \frac{EA\alpha\Delta\theta}{1-2v} \right) \phi(x) \left(\frac{d^2\phi}{dx^2} - (e_o a)^2 \frac{d^4\phi}{dx^4} \right) dx$$

For the undamped clamped-clamped, clamped-simple and simple-simple supported structures, *G=0* and Equation (9) reduces to

$$M\ddot{u}(\tau) + (K + C)u(\tau) - Vu^3(\tau) = 0 \tag{31}$$

which can be written as

$$\ddot{u}(\tau) + \alpha u(\tau) + \beta u^3(\tau) = 0 \tag{32}$$

where

$$\alpha = \frac{(K+C)}{M}, \beta = -\frac{V}{M}$$

Method of solution by homotopy perturbation method

Application of regular perturbation to the nonlinear Equation (32) breaks down at the time t of $O(\varepsilon^{-2})$. Also, the traditional perturbation methods (regular and singular perturbation methods) are based on the existence of small parameter in the nonlinear equations and such are limited to analysis of weakly nonlinear equation. Unfortunately, the nonlinear equation as shown in Equation (32) does not have any small perturbation and it is strongly nonlinear. Therefore, in this work, homotopy perturbation method is used to solve the equation. The homotopy perturbation method eliminates the "the small parameter assumption" as carried in the traditional perturbation

methods. It is a powerful method that gives acceptable analytical results with convenient convergence and stability [16-20].

The basic idea of homotopy perturbation method

In order to establish the basic idea behind homotopy perturbation method, consider a system of nonlinear differential equations given as,

$$A(U) - f(r) = 0, \quad r \in \Omega \tag{33}$$

with the boundary conditions

$$B\left(u, \frac{\partial u}{\partial \eta}\right) = 0, \qquad r \in \Gamma \tag{34}$$

where A is a general differential operator, B is a boundary operator, $f(r)$ a known analytical function and Γ is the boundary of the domain Ω

The operator A can be divided into two parts, which are L and N, where L is a linear operator, N is a non-linear operator. Equation (13) can be therefore rewritten as follows;

$$L(u) + N(u) - f(r) = 0 \tag{35}$$

By the homotopy technique, a homotopy $U(r,p): \Omega \times [0,1] \to R$ can be constructed, which satisfies

$$H(U,p) = (1-p)\left[L(U) - L(U_o)\right] + p\left[A(U) - f(r)\right] = 0, \quad p \in [0,1] \tag{36}$$

Or

$$H(U,p) = L(U) - L(U_o) + pL(U_o) + p\left[N(U) - f(r)\right] = 0 \tag{37}$$

In the above Equations (36) and (37), $p \in [0,1]$ is an embedding parameter, u_o is an initial approximation of equation of Equation (33), which satisfies the boundary conditions.

Also, from Equations (36) and (37), we will have,

$$H(U,0) = L(U) - L(U_o) = 0 \tag{38}$$

$$H(U,0) = A(U) - f(r) = 0 \tag{39}$$

The changing process of p from zero to unity is just that of $U(r,p)$ from $u_o(r)$ to $u(r)$. This is referred to homotopy in topology. Using the embedding parameter p as a small parameter, the solution of Equations (36) and (37) can be assumed to be written as a power series in p as given in Equation (40)

$$U = U_o + pU_1 + p^2 U_2 + \dots \tag{40}$$

It should be pointed out that of all the values of p between 0 and 1, $p=1$ produces the best result. Therefore, setting $p = 1$, results in the approximation solution of Equation (33)

$$u = \lim_{p \to 1} U = U_o + U_1 + U_2 + ... \quad (41)$$

The basic idea expressed above is a combination of homotopy and perturbation method. Hence, the method is called homotopy perturbation method (HPM), which has eliminated the limitations of the traditional perturbation methods. On the other hand, this technique can have full advantages of the traditional perturbation techniques. The series Equation (41) is convergent for most cases.

Application of the homotopy perturbation method to the present problem

According to homotopy perturbation method (HPM), we can construct an homotopy for Equation (32) as

$$H(U, p) = (1 - p)\left[\ddot{U} + \alpha U\right] + p\left[\ddot{U} + \alpha U + \beta U^3\right] = 0, \quad p \in [0,1] \quad (42)$$

Or equivalently,

$$\ddot{U} + \alpha U + p\beta U^3 = 0 \quad (43)$$

Supposing that the solution of Equation (33) can be expressed in a series in p:

$$U = U_0 + pU_1 + p^2 U_2 + ... \quad (44)$$

According to HPM, a constant can be expanded as a power series of the embedding parameter p.
So, constant α can be expanded as;

$$\alpha = \omega_0^2 + p\omega_1^2 + p^2 \omega_2^2 + ... \quad (45)$$

On substituting Equation (44) and (45) into Equation (43), an approximate solution for Equation (43) can be expressed as:

$$\left(\ddot{U}_0 + p\ddot{U}_1 + p^2 \ddot{U}_2 + ...\right) + \left(\omega_0^2 + p\omega_1^2 + p^2 \omega_2^2 + ...\right)\left(U_0 + pU_1 + p^2 U_2 + ...\right) +$$
$$p\beta\left(U_0 + pU_1 + p^2 U_2 + ...\right)^3 = 0 \quad (46)$$

Expanding the above Equation (46) and collecting all terms with the same order of p together, the resulting equation appears in form of polynomial in p. On equating each coefficient of the resulting polynomial in p to zero, we arrived at a set of differential equations u_i and ω_i^2 $(i = 0, 1, 2,...)$

$$p^0: \quad \ddot{U} + \omega_0^2 U_0 = 0 \quad (47a)$$

$$p^1: \quad \ddot{U}_1 + \omega_0^2 U_1 + \omega_2^2 U_0 + \beta U_0^3 = 0 \quad (47b)$$

$$p^2: \quad \ddot{U}_2 + \omega_0^2 U_2 + \omega_1^2 U_1 + \omega_2^2 U_0 + 3\beta U_0^3 U_1 = 0 \quad (47c)$$

where the initial conditions for u_i satisfy:

$$U_0(0) = a, \quad \dot{U}_0(0) = 0, \; U_i(0) = 0, \quad \dot{U}_i(0) = 0, \quad (i = 1, 2,...) \quad (48)$$

Using the initial conditions in Equation (28), Equation (27a) can easily be solved and the solution gives

$$U_0 = a \cos \omega_0 t \tag{49}$$

Substituting the solution of U_0 in Equation (29) into Equation (27b), we have

$$\ddot{U}_1 + \omega_0^2 U_1 + \left(\omega_1^2 a + \frac{3a^3 \beta}{4} \right) \cos \omega_0 t + \frac{a^3 \beta}{4} \cos 3\omega_0 t = 0 \tag{50}$$

On eliminating the secular term that appeared in Equation (30), we arrived at

$$\omega_1^2 = -\frac{3a^2 \beta}{4} \tag{51}$$

After eliminating the secular term, on solving Equation (47b) under the initial conditions of Equation (48), the solution for U_1 is

$$U_1 = \frac{a^3 \beta}{32 \omega_0^2} \left(\cos 3\omega_0 t - \cos \omega_0 t \right) \tag{52}$$

Again, on substituting Equation (29) and (32) into Equation (27c), we have

$$\ddot{U}_2 + \omega_0^2 U_2 + \left(a\omega_2^2 - \frac{3a^5 \beta^2}{64 \omega_0^2} - \frac{a^3 \beta \omega_1^2}{32 \omega_0^2} \right) \cos \omega_0 t + \left(\frac{a^3 \beta \omega_1^2}{32 \omega_0^2} + \frac{3a^5 \beta^2}{128 \omega_0^2} \right) \cos 3\omega_0 t + \frac{3a^5 \beta^2}{128 \omega_0^2} \cos 5\omega_0 t = 0 \tag{53}$$

If we eliminate the secular term in Equation (53), we have

$$\omega_2^2 = \frac{3a^4 \beta^2}{64 \omega_0^2} + \frac{a^2 \beta \omega_1^2}{32 \omega_0^2} \tag{54}$$

Substituting Equation (51) into Equation (54), we have

$$\omega_2^2 = \frac{3a^4 \beta^2}{128 \omega_0^2} \tag{55}$$

Again, after eliminating the secular term of Equation (53), on solving the resulting Equation (53) using the initial conditions in Equation (48), we arrived at

$$U_2 = \frac{a^5 \beta^2}{1024 \omega_0^4} \left(\cos 5\omega_0 t - \cos \omega_0 t \right) \tag{56}$$

From Equation (24) and (45), if only the first-order approximate solution are searched for, when $p=1$, we have the first-order approximate frequency and displacement solution as

$$\omega_{0,1th} = \omega_0 = \sqrt{\alpha - \omega_1^2} = \sqrt{\alpha + \frac{3a^2\beta}{4}} \tag{57}$$

$$U_{1th} = a\cos\omega_0 t + \frac{a^3\beta}{32\omega_0^2}\left(\cos 3\omega_0 t - \cos\omega_0 t\right) \tag{58}$$

If only the second-order approximate solution is searched for, when $p=1$, from Equation (44) and (45), we have the second-order approximately frequency and displacement solution

$$\omega_{0,2th} = \omega_0 = \frac{\sqrt{2}}{2}\sqrt{\alpha + \frac{3a^2\beta}{4} - \sqrt{\left(\alpha + \frac{3a^2\beta}{4}\right)^2 - \frac{3a^4\beta^2}{32}}} \tag{59}$$

$$U_{2th} = \left(a - \frac{a^3\beta}{32\omega_0^2} - \frac{a^3\beta^2}{1024\omega_0^4}\right)\cos\omega_0 t + \frac{a^3\beta}{32\omega_0^2}\cos 3\omega_0 t + \frac{a^5\beta^2}{1024\omega_0^4}\cos 5\omega_0 t \tag{60}$$

Alternatively, if we substitute Equations (49), (52) and (56) into Equation (44), we have

$$U = a\cos\omega_0 t + p\left[\frac{a^3\beta}{32\omega_0^2}\left(\cos 3\omega_0 t - \cos\omega_0 t\right)\right] + p^2\left[\frac{a^5\beta^2}{1024\omega_0^4}\left(\cos 5\omega_0 t - \cos\omega_0 t\right)\right] + \dots \tag{61}$$

Setting $p=1$, results in the approximation solution of Equation (61) and we have

$$u(t) = \left(a - \frac{a^3\beta}{32\omega_0^2} - \frac{a^5\beta^2}{1024\omega_0^4}\right)\cos\omega_0 t + \frac{a^3\beta}{32\omega_0^2}\cos 3\omega_0 t + \frac{a^5\beta^2}{1024\omega_0^4}\cos 5\omega_0 t + \dots \tag{62}$$

The trial/comparison functions, $\phi(x)$ for different supports/boundary conditions are defined in Equations (7), (11), (14), (17), (18), (21), (22), (23) and (26).

Clamped-Clamped (doubly clamped)
The approximate analytical solution is

$$w(x,t) \approx \left\{ \begin{array}{c} \left(a - \dfrac{a^3\beta}{32\omega_0^2} - \dfrac{a^5\beta^2}{1024\omega_0^4}\right)\cos\omega_0 t \\ + \dfrac{a^3\beta}{32\omega_0^2}\cos 3\omega_0 t + \dfrac{a^5\beta^2}{1024\omega_0^4}\cos 5\omega_0 t \end{array} \right\} \left[\begin{array}{c} cosh\lambda_n x - cos\lambda_n x \\ -\left(\dfrac{cosh\lambda_n L - cos\lambda_n L}{sinh\lambda_n L - sin\lambda_n L}\right)\left(sinh\lambda_n x - sin\lambda_n x\right) \end{array} \right] \tag{63}$$

Or

$$w(x,t) \approx \left\{ \begin{array}{l} \left(a - \dfrac{a^3\beta}{32\omega_0^2} - \dfrac{a^5\beta^2}{1024\omega_0^4} \right)\cos\omega_0 t \\[2mm] + \dfrac{a^3\beta}{32\omega_0^2}\cos 3\omega_0 t + \dfrac{a^5\beta^2}{1024\omega_0^4}\cos 5\omega_0 t \end{array} \right\} \left[\begin{array}{l} cosh\lambda_n x - cos\lambda_n x \\[2mm] -\left(\dfrac{sinh\lambda_n L - sin\lambda_n L}{cosh\lambda_n L - cos\lambda_n L} \right)(sinh\lambda_n x - sin\lambda_n x) \end{array} \right] \quad (64)$$

where λ_n are the roots of the equation $cos\lambda_n L cosh\lambda_n L = 1$

Clamped-Simple supported

The approximate analytical solution is

$$w(x,t) \approx \left\{ \begin{array}{l} \left(a - \dfrac{a^3\beta}{32\omega_0^2} - \dfrac{a^5\beta^2}{1024\omega_0^4} \right)\cos\omega_0 t \\[2mm] + \dfrac{a^3\beta}{32\omega_0^2}\cos 3\omega_0 t + \dfrac{a^5\beta^2}{1024\omega_0^4}\cos 5\omega_0 t \end{array} \right\} \left[\begin{array}{l} cosh\lambda_n x - cos\lambda_n x \\[2mm] -\left(\dfrac{cosh\lambda_n L - cos\lambda_n L}{sinh\lambda_n L - sin\lambda_n L} \right)(sinh\lambda_n x - sin\lambda_n x) \end{array} \right] \quad (65)$$

λ_n are the roots of the equation $tan\lambda_n L = tanh\lambda_n L$

Simple-Simple supported

$$w(x,t) \approx \left\{ \begin{array}{l} \left(a - \dfrac{a^3\beta}{32\omega_0^2} - \dfrac{a^5\beta^2}{1024\omega_0^4} \right)\cos\omega_0 t \\[2mm] + \dfrac{a^3\beta}{32\omega_0^2}\cos 3\omega_0 t + \dfrac{a^5\beta^2}{1024\omega_0^4}\cos 5\omega_0 t \end{array} \right\} sin\dfrac{n\pi x}{L} \quad (66)$$

Clamp-Free (cantilever)

$$w(x,t) \approx \left\{ \begin{array}{l} \left(a - \dfrac{a^3\beta}{32\omega_0^2} - \dfrac{a^5\beta^2}{1024\omega_0^4} \right)\cos\omega_0 t \\[2mm] + \dfrac{a^3\beta}{32\omega_0^2}\cos 3\omega_0 t + \dfrac{a^5\beta^2}{1024\omega_0^4}\cos 5\omega_0 t \end{array} \right\} \left[\begin{array}{l} cosh\lambda_n x - cos\lambda_n x \\[2mm] -\left(\dfrac{cosh\lambda_n L + cos\lambda_n L}{sinh\lambda_n L + sin\lambda_n L} \right)(sinh\lambda_n x - sin\lambda_n x) \end{array} \right] \quad (67)$$

Or

$$w(x,t) \approx \left\{ \begin{array}{l} \left(a - \dfrac{a^3\beta}{32\omega_0^2} - \dfrac{a^5\beta^2}{1024\omega_0^4} \right)\cos\omega_0 t \\[2mm] + \dfrac{a^3\beta}{32\omega_0^2}\cos 3\omega_0 t + \dfrac{a^5\beta^2}{1024\omega_0^4}\cos 5\omega_0 t \end{array} \right\} \left[\begin{array}{l} cosh\lambda_n x - cos\lambda_n x \\[2mm] -\left(\dfrac{sinh\lambda_n L - sin\lambda_n L}{cosh\lambda_n L - cos\lambda_n L} \right)(sinh\lambda_n x - sin\lambda_n x) \end{array} \right] \quad (68)$$

λ_n are the roots of the equation $cos\lambda_n L cosh\lambda_n L = -1$

where in all the solutions shown above,

$$\omega_0 = \frac{\sqrt{2}}{2}\sqrt{\alpha + \frac{3a^2\beta}{4} - \sqrt{\left(\alpha + \frac{3a^2\beta}{4}\right)^2 - \frac{3a^4\beta^2}{32}}}, \quad \alpha = \frac{(K+C)}{M}, \quad \beta = -\frac{V}{M}$$

and

$$M = \int_0^L (m_p + m_f)\phi(x)\left(\phi(x) - (e_o a)^2 \frac{d^2\phi}{dx^2}\right) + \phi(x)\left(m_f u^2 \phi(x) - (e_o a)^2 \frac{d^2\phi}{dx^2}\right) dx$$

$$G = \int_0^L \phi(x)\left\{\left(2m_f v \frac{d\phi}{dx} - (e_o a)^2 \frac{d^3\phi}{dx^3}\right) + \left(\mu\phi(x) - (e_o a)^2 \frac{d^2\phi}{dx^2}\right)\right\} dx$$

$$K = \int_0^L \phi(x)\left\{EI \frac{d^4\phi}{dx^4} + k_1\phi(x) - k_p \frac{d^2\phi}{dx^2} - k_1(e_o a)^2 \frac{d^2\phi}{dx^2} + (e_o a)^2 k_p \frac{d^2\phi}{dx^2}\right\} dx$$

$$C = \int_0^L \left(m_f u^2 + PA - T - \frac{EA\alpha\Delta\theta}{1-2v}\right)\phi(x)\left(\frac{d^2\phi}{dx^2} - (e_o a)^2 \frac{d^4\phi}{dx^4}\right) dx$$

$$V = \int_0^L \phi(x)\left\{\begin{array}{l}\left[N_o + \frac{EA}{2L}\int_0^L \left(\frac{\partial\phi}{\partial x}\right)^2 dx\right]\frac{d^2\phi}{dx^2} - k_3\frac{d^3\phi}{dx^3}(x) + 6k_3(e_o a)^2 \phi(x)\left(\frac{\partial\phi}{\partial x}\right)^2 \\ -3k_3(e_o a)^2 \phi^2(x)\frac{\partial\phi}{\partial x} - (e_o a)^2\left[N_o + \frac{EA}{2L}\int_0^L\left(\frac{\partial\phi}{\partial x}\right)^2 dx\right]\frac{d^4\phi}{dx^4}\end{array}\right\} dx$$

While for the slightly curved nanotube, *M, G, K* and *C* are the same as above but

$$V = \int_0^L \phi(x)\left\{\begin{array}{l}\left[N_o + \frac{EA}{2L}\int_0^L\left\{\frac{\partial Z_o}{\partial x}\frac{\partial w}{\partial x} + \left(\frac{\partial w}{\partial x}\right)^2\right\}dx\right]\left[\frac{\partial^2 w}{\partial x^2} + \frac{\partial^2 Z_o}{\partial x^2}\right] - k_3\frac{d^3\phi}{dx^3}(x) + 6k_3(e_o a)^2 \phi(x)\left(\frac{\partial\phi}{\partial x}\right)^2 \\ -3k_3(e_o a)^2 \phi^2(x)\frac{\partial\phi}{\partial x} - (e_o a)^2\left[N_o + \frac{EA}{2L}\int_0^L\left\{\frac{\partial Z_o}{\partial x}\frac{\partial w}{\partial x} + \left(\frac{\partial w}{\partial x}\right)^2\right\}dx\right]\left[\frac{\partial^4 w}{\partial x^4} + \frac{\partial^4 Z_o}{\partial x^4}\right]\end{array}\right\} dx$$

It should be noted that the definitions and the values *M, K, C*, and *V* are trial/shape function-dependent. Therefore, they are different for the different boundary conditions considered. Also, by extension, the values of α and β in the solutions are different for the different supports analyzed.

RESULTS AND DISCUSSION

Based on the shape functions defined in Equations (7), (14), (18), (22) and (23), the first five normalized mode shapes of the beams for clamped-clamped, simple-simple, clamped-simple and clamped-free supports are shown in Figure. 2-5. Also, the figures depict the deflections of the beams along the beams' span at five different buckled and mode shapes.

Following to the polynomial functions developed in this work in Equations (11), (17), (21) and (26) for the hyperbolic-trigonometric functions defined in Equations (7), (14), (18), (22) and (23), Figures 6-9 show the comparison of hyperbolic-trigonometric and the polynomial functions for the normalized mode shapes of the beams for clamped-clamped, simple-simple, clamped-simple and clamped-free supports. The figures depict the validity of the developed polynomial functions in this work as there are very good agreements between the hyperbolic-trigonometric and the developed polynomial functions.
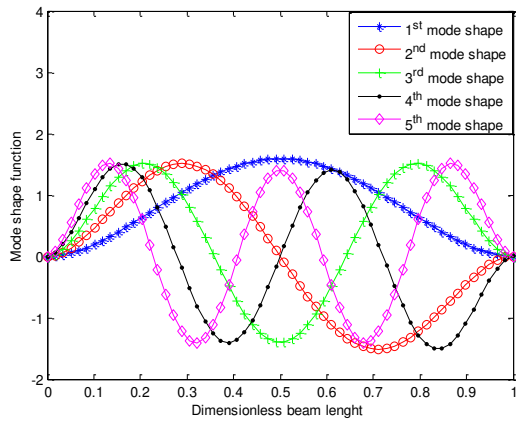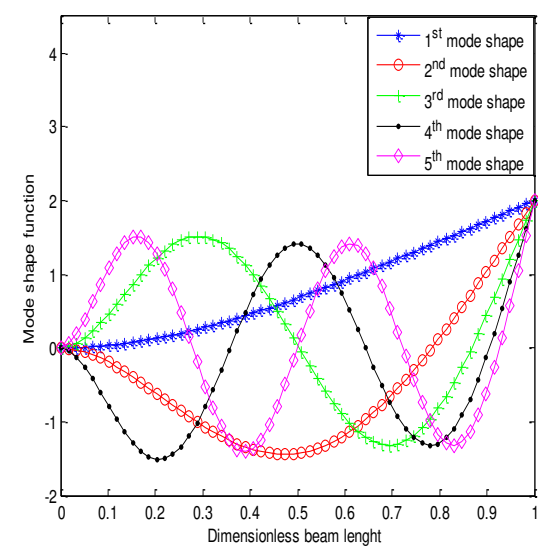
**Figure 2.** The first five normalized mode shaped of the beams under clamped-clamped supports
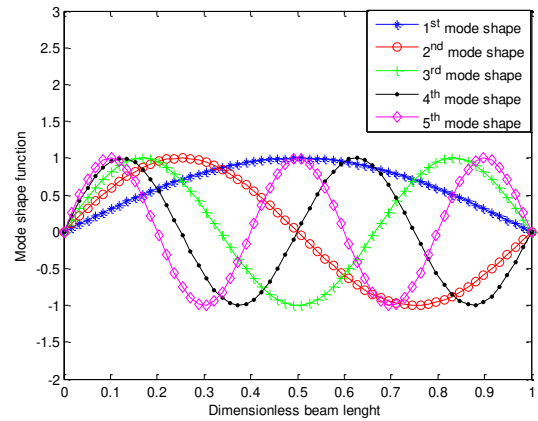
Figure 3. The first five normalized mode shaped of the beams under simple-simple supports
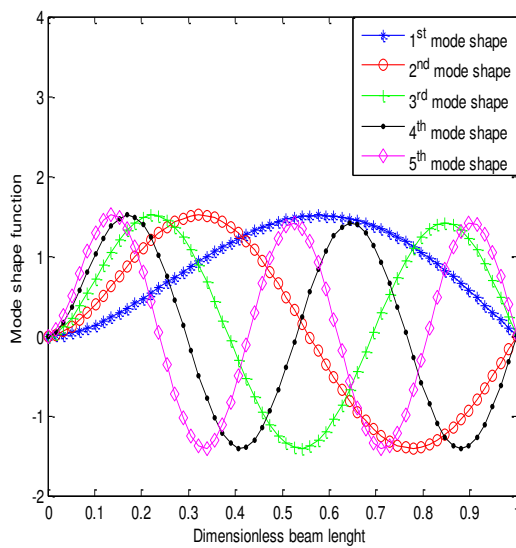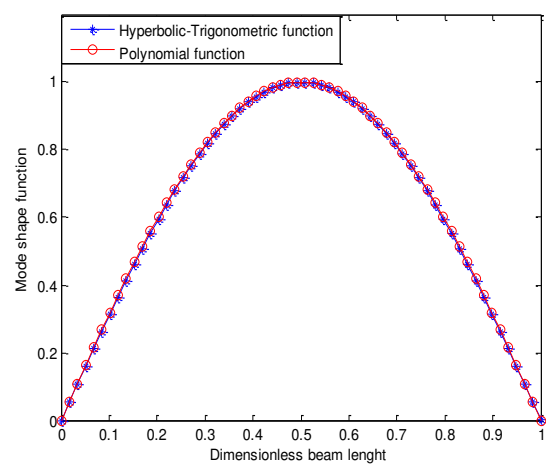

Figure 4. The first five normalized mode shaped of the beams mode shaped of the under clamped-simple supports
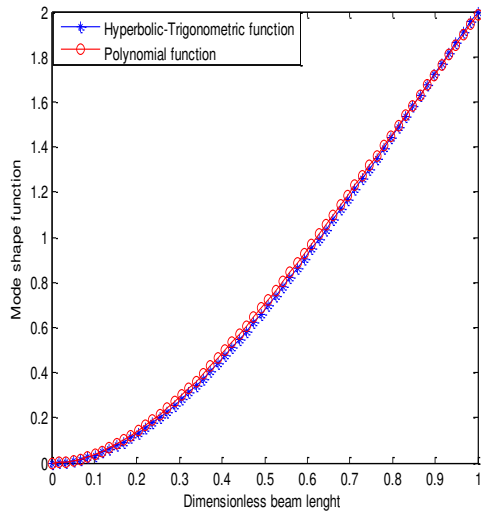

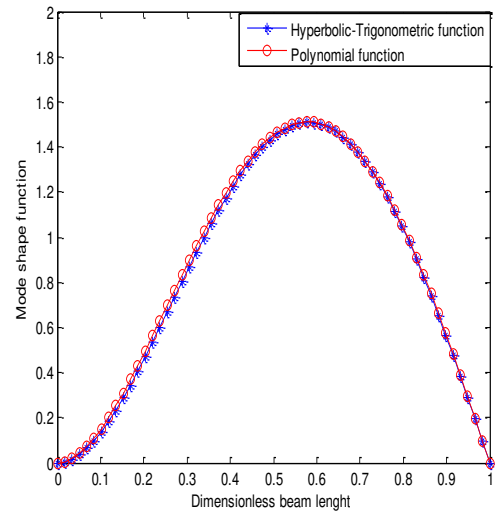**Figure 5.** The first five normalized beams under clamped-free (cantilever) supports
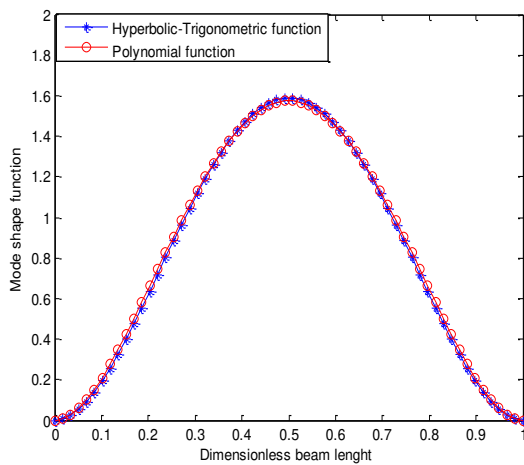
Figure 6. Normalized mode shaped of the structures under clamped-clamped supports for Hyperbolic-Trigonometric and Polynomial functions

Figure 7. Normalized mode shaped of the structures under simple-supports for Hyperbolic-Trigonometric and Polynomial functions

Figure 8. Normalized mode shaped of the structures under clamped-free supports for Hyperbolic-Trigonometric and Polynomial functions

Figure 9. Normalized mode shaped of the structures under clamped- pinned supports for Hyperbolic-Trigonometric and Polynomial functions

Figure 10 illustrates the effects of boundary conditions on the nonlinear amplitude-frequency response curves of the nanotube. Also, the figure shows the variation of frequency ratio of the nanotube with the dimensionless maximum amplitude of the structure under different boundary conditions. From, the result, it shown that frequency ratio is highest in the beam which is clamped-free (cantilever) supported beam and lowest with clamped-clamped beam. The lowest frequency ratio of the clamped-clamped beam is due to high stiffness of the beam with this type of boundary conditions in comparison with other types of boundary conditions.
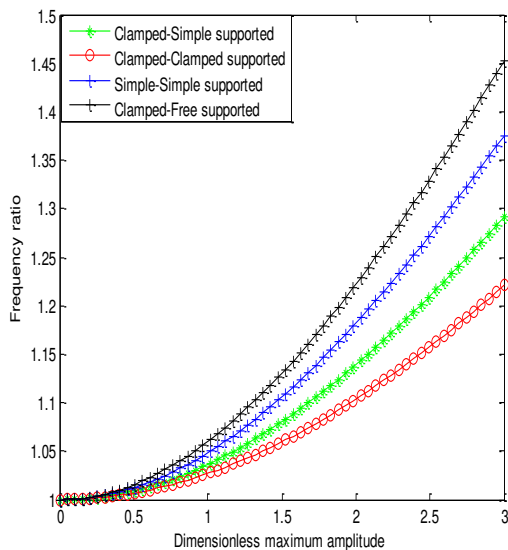
Figure 10. Effects of boundary conditions on the nonlinear amplitude-frequency response curves of the nanotube
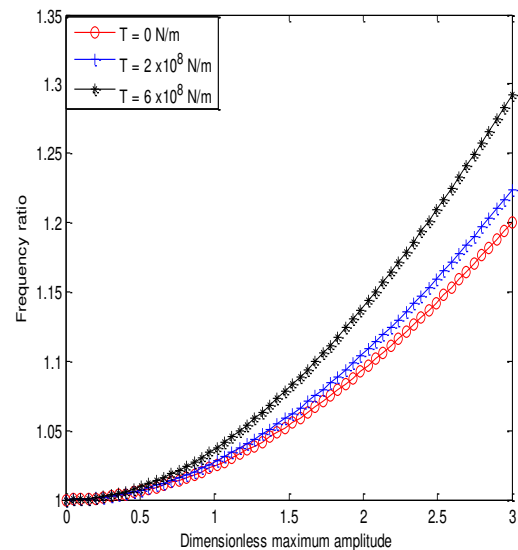
Figure 11. Effects of axial tension on the nonlinear amplitude-frequency response curves of SWCNT

Figure 11 shows effects of axial tension on the nonlinear amplitude-frequency response curves of pipe. It is observed that the increase of axial tension, the nonlinear vibration frequencies increases. It can be seen from the figure, in contrast to linear systems, the nonlinear frequency is a function of amplitude so that the larger the amplitude, the more pronounced the discrepancy between the linear and the nonlinear frequencies becomes.
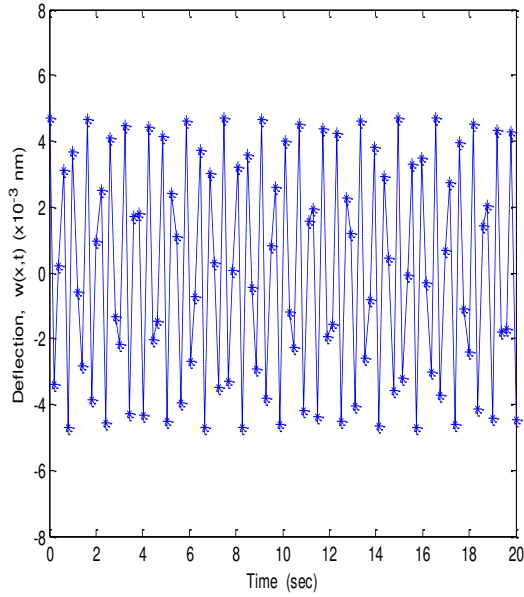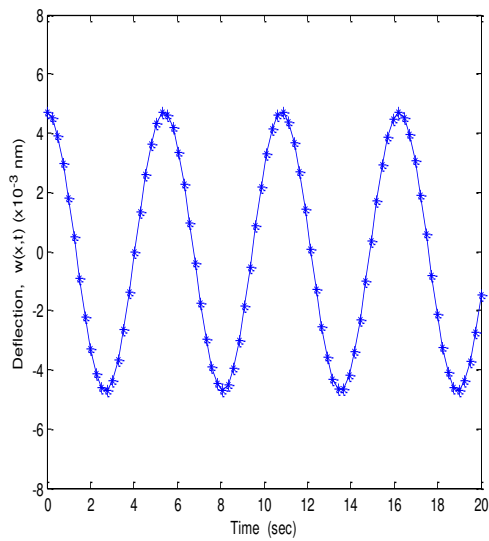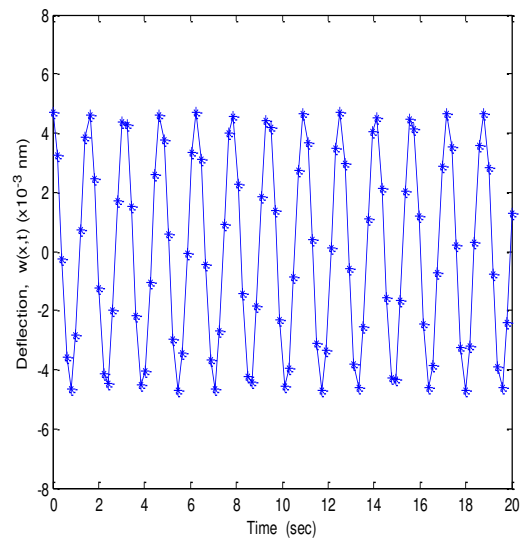
Figure 12. Midpoint deflection time history for the nonlinear analysis of SWCBT when Kn=0.00 and U= 500 m/s
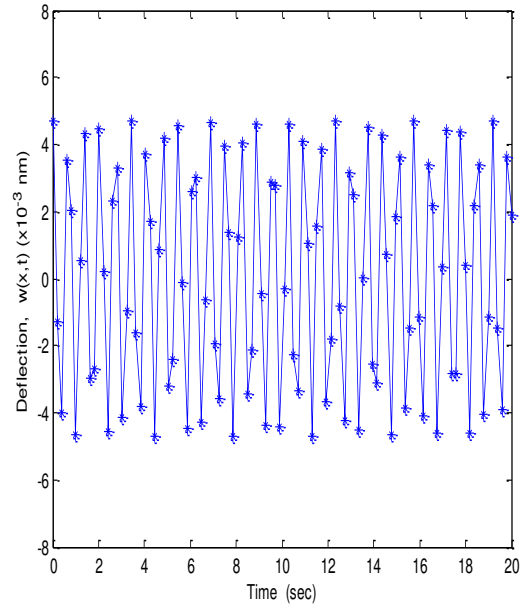
**Figure 13.** Midpoint deflection time history for the nonlinear analysis of SWCBT when Kn=0.01 and U= 500 m/s

**Figure 14.** Midpoint deflection time history for the nonlinear analysis of SWCBT when Kn=0.03 and U= 100 m/s

Figure 15. Midpoint deflection time history for the nonlinear analysis of SWCBT when Kn=0.03 and U= 500 m/s

Figure 12 shows the midpoint deflection time history of the SWCBT under no slip condition while Figure 13, 14 and 15 shows the effects of slip on the dynamic behavior of the nanotube. Figure 14 illustrates the midpoint deflection time history for the nonlinear analysis of SWCBT when *Kn=0.03* and *U= 100 m/s* while Figure 15 presents the midpoint deflection time history for the nonlinear analysis of SWCBT when *Kn=0.03* and *U= 500 m/s*.
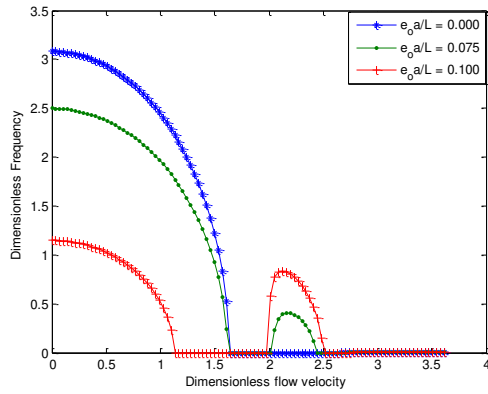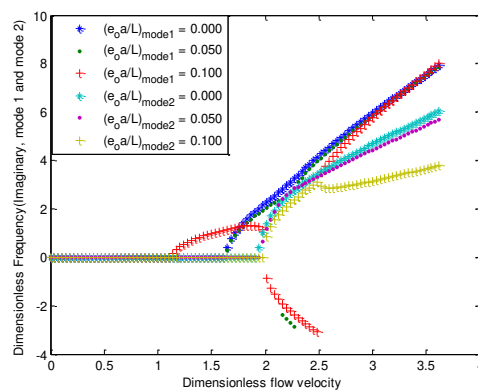
Figure 16. Effects of nonlocal parameter on the natural frequency of the nonlinear vibration
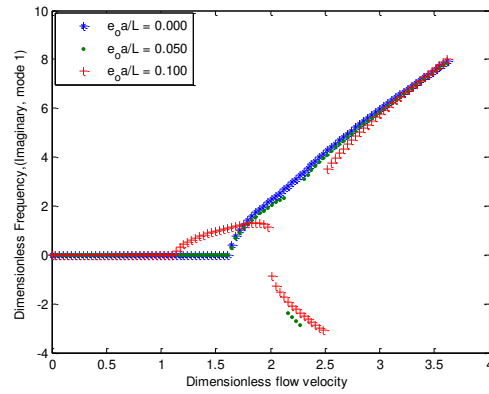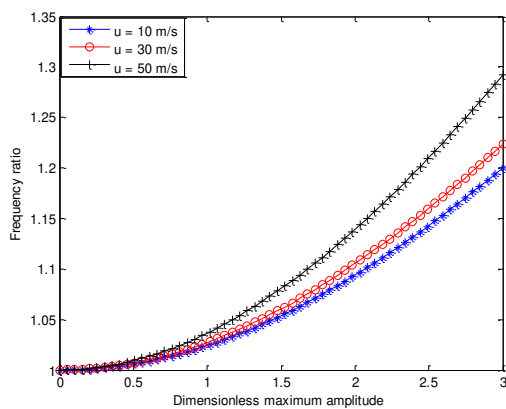

Figure 17. Effects of nonlocal parameter on the natural frequency of the nonlinear vibration
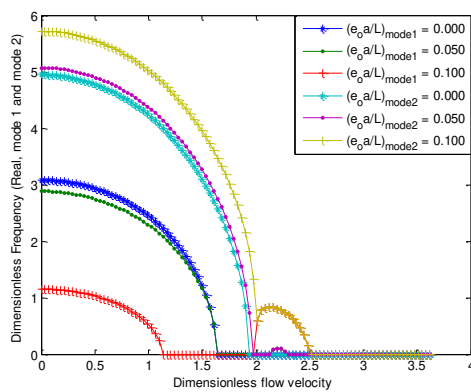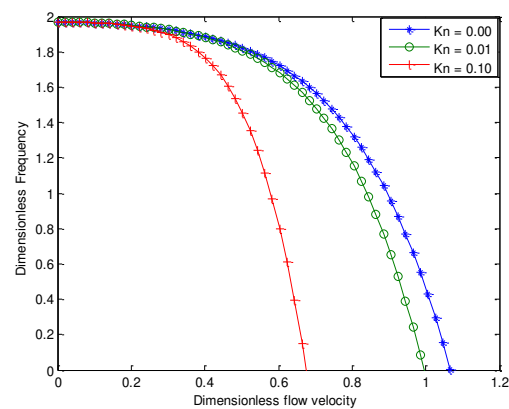

Figure 18. Effects of nonlocal parameter on the natural frequency of the nonlinear vibration for first and second modes

Figure 19. Effects of nonlocal parameter on the natural frequency of the nonlinear vibration for first and second modes

Figure 20. Effects of flow-velocity on the natural frequency of the structure vibration


Figure 21. Effects of Knudsen number on the dimensionless frequency of simply supported single-walled nanotube

The studies and the investigations of the dynamic and stability behaviours of the structure are largely dependent on the effects of fluid flow velocity, amplitude on the natural frequencies of the vibration. Effects of nonlocal parameter, velocity and temperature on the vibration of the nanotube are shown in Figure 16-21. It is depicted that increase in the slip parameter leads to decrease in the frequency of vibration of the structure and the

critical velocity of the conveyed fluid. It should be pointed out as shown in the figures that the zero value for the nonlocal parameter, i.e. $e_o a = 0$, represents the results of the classical Euler-Bernoulli model which has the highest frequency and critical fluid velocity (a point where the structure starts to experience instability). When the flow velocity of the fluid attains the critical velocity, both the real and imaginary parts of the frequency are equal to zero. Also, the figures present the critical speeds corresponding to the divergence conditions for different values of the nonlocal parameters. It is shown in Figures 16, 17, 18, 19 and 20, the real and imaginary parts of the eigenvalues related to the two lowest modes with different nanotube parameters. Effects of slip parameter, Knudsen number on the dimensionless frequency ratio of the nanotube are shown in Figures 21. It is depicted that increase in the slip parameter leads to decrease in the dimensionless frequency ratio of vibration of the SWCNT. It should be pointed out that the Knudsen number predicts various flow regimes in the fluid-conveying nanotube. The Knudsen number with zero value has the highest frequency as shown in the figure. As the Knudsen number increases, the bending stiffness of the nanotube decreases and in consequent, the critical continuum flow velocity decreases as the curves shift to the lowest frequency zone.

Effects of change in temperature on the natural frequencies are given shown in Figures 22 and 23. As the change in temperature increases, the natural frequencies and the critical flow velocity of the structure increase for the low or room temperature while at high temperature, increase in temperature change, decreases the natural frequencies and the critical flow velocity of the structure.
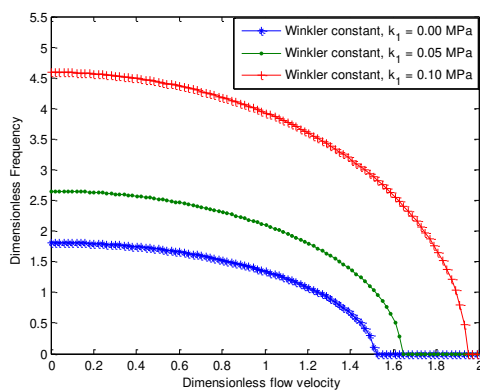
Effects of elastic foundation parameters on the vibration of the nanotube are shown in Figures 24-27. It is depicted that increase in the Winkler and Pasternak foundation parameters increases the frequency of vibration of the structure and the critical velocity of the conveyed fluid.
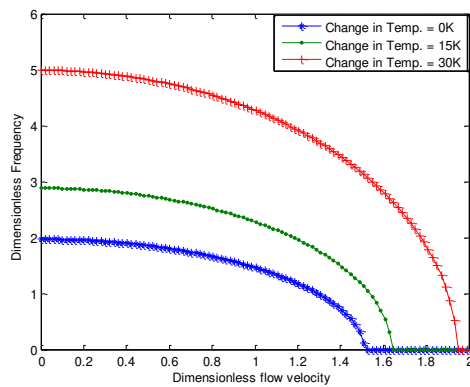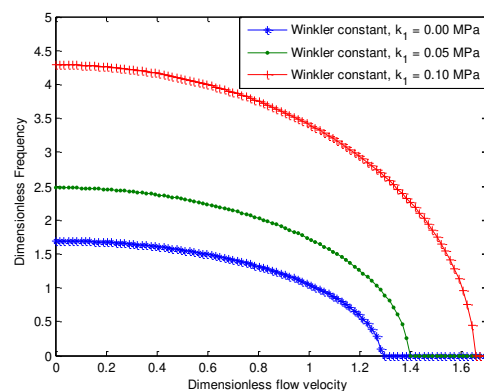

Figure 22. Effects of change in temperature on the natural frequency of the nonlinear vibration at low temperature
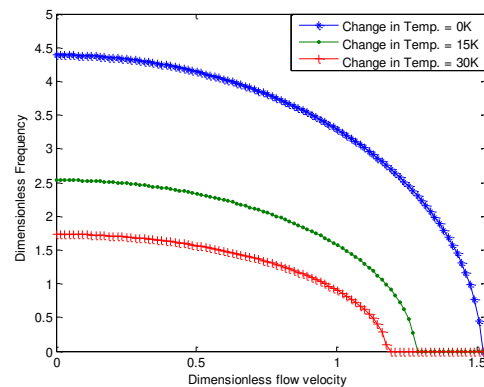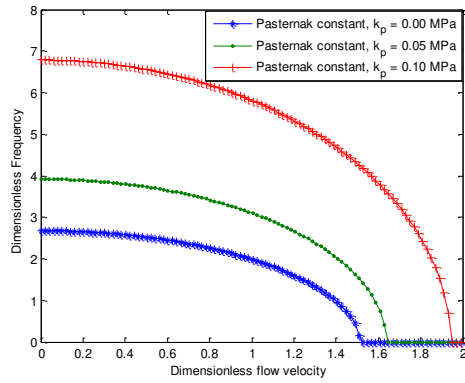

Figure 23. Effects of change in temperature on the natural frequency of the nonlinear vibration at high temperature
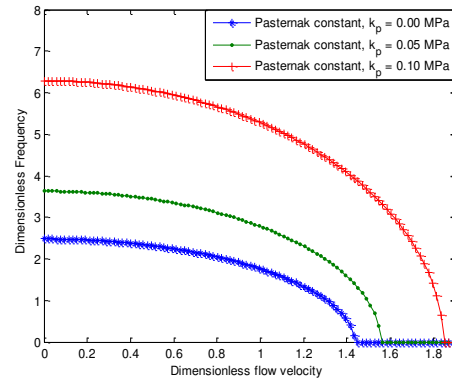

Figure 24. Effects of Winkler foundation parameter on the natural frequency of the nonlinear vibration at low temperature


Figure 25. Effects of Winkler foundation parameter on the natural frequency of the nonlinear vibration at high temperature
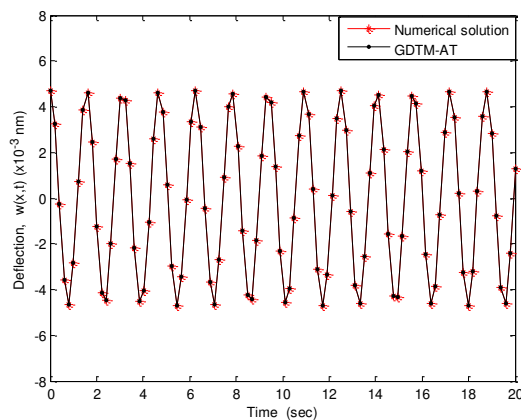
Figure 26. Effects of Pasternak foundation parameter on the natural frequency of the nonlinear vibration at low temperature

Figure 27. Effects of Pasternak foundation parameter on the natural frequency of the nonlinear vibration at high temperature
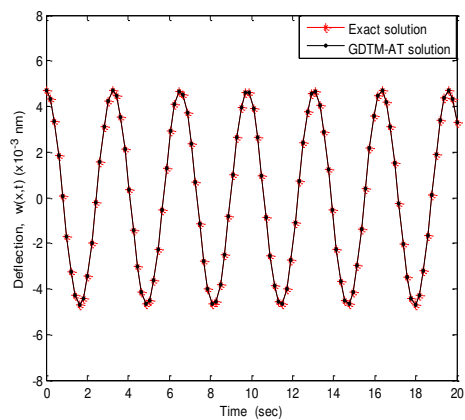
Figure 28. Comparison between the obtained results and the exact solution for the linear vibration

Figure 29. Comparison between the obtained results and the numerical solution for the nonlinear vibration

In order to verify the model, Figures 18 and 19 show the comparison of the results of exact analytical solution and the results of the present study for the linear models while Figure 13 presents the comparison of numerical results models and the results of present work for the nonlinear models. The results show that good agreements are established between the solutions.

CONCLUSION

In this work, thermo-fluidic parameter effects on the nonlinear vibration of carbon nanotube conveying fluid under elastic foundations has been investigated using homotopy perturbation method. From the analysis it is established that increase in the Knudsen number, the slip parameter, leads to decrease in the frequency of vibration and the critical velocity while natural frequency and the critical fluid velocity increase as the in stretching effect increases. Also, as the Knudsen number increases, the bending stiffness of the nanotube decreases and in consequent, the critical continuum flow velocity decreases as the curves shift to the lowest frequency zone. As the change in temperature increases, the natural frequencies and the critical flow velocity of the structure increase for the low or room temperature while at high temperature, increase in temperature change, decreases the natural frequencies and the critical flow velocity of the structure. Further, it is established that the alteration of nonlinear flow-induced frequency from linear frequency is significant as the amplitude, flow velocity, and aspect ratio increase. The analytical solutions can serve as benchmarks for other methods of solutions of the problem. They can also provide a starting point for a better understanding of the relationship between the physical quantities of the problems.

NOMENCLATURE

A	Area of the structure
E	Young Modulus of Elasticity
G	Shear Modulus
I	moment of area
kp	Pasternak foundation coefficient
k1	linear Winkler foundation coefficient
k3	nonlinear Winkler foundation coefficient
Kn	Knudsen number,
lo,	l1, l2 independent length scale parameters
L	length
Mp	mass of the structure
mf	mass of fluid
N	axial/Longitudinal force
P	Pressure
r	radius of the structure
t	time
T	tension
$u(t)$	generalized coordinate of the system
w	transverse displacement/deflection
x	axial coordinate
Zo(x)	is the arbitrary initial rise function.
Σv	tangential moment accommodation coefficient
$\phi(x)$	trial/comparison function
υ	Poisson' ratio
μ	damping coefficient
Δθ	change in temperature
α	coefficient of expansion

REFERENCES

[1] Iijima, S. (1991). Helical microtubules of graphitic carbon", Nature, London, 354, 6348, 56–58.

[2] Yoon, C., Ru, C. Q. and Mioduchowski, A. (2005). Vibration and instability of carbon nanotubes conveying fluid", Journal of Applied Mechanics, Transactions of the ASME, 65(9), 1326–1336.

[3] Yan, Y, Wang, W. Q. and Zhang, L. X. (2010). Nonlocal effect on axially compressed buckling of triple-walled carbon nanotubes under temperature field. Journal of Applied Math and Modelling, 34, 3422–3429.

[4] Murmu, T. and Pradhan, S. C. (2009). Thermo-mechanical vibration of Single-walled carbon nanotube embedded in an elastic medium based on nonlocal elasticity theory", Computational Material Science, 46, 854–859.

[5] Yang, H. K. and Wang, X. (2006). Bending stability of multi-wall carbon nanotubes embedded in an elastic medium", Modeling and Simulation in Materials Sciences and Engineering, 14, 99–116.

[6] Yoon, J., Ru, C. Q and Mioduchowski, A. (2003). Vibration of an embedded multiwall carbon nanotube", Composites Science and Technology, 63(11), 1533–1542.

[7] Ghorbanpour, Arani, A. Dashti, P., Amir, S. and Yousefi, M. (2005). Nonlinear vibration of coupled nano- and microstructures conveying fluid based on Timoshenko beam model under two-dimensional magnetic field. Acta Mechanica, 226, 2729-2760.

[8] Choi, J., Song, O. and Kim, S. (2013). Nonlinear stability characteristics of carbon nanotubes conveying fluids, Acta Mechanica, 224, 1383-1396.

[9] Zhang, D. P., Lei, Y. and Shen, Z. B. (2016). Free transverse vibration of double-walled carbon nanotubes embedded in viscoelastic medium. Acta Mechanica, 227, 3657-3670.

[10] Kiani, K. (2013). Characterization of free vibration of elastically supported double-walled carbon nanotubes subjected to a longitudinally varying magnetic field. Acta Mechanica, 224, 3139-3151.

[11] Kiani, K. (2011). Application of nonlocal beam models to double-walled carbon nanotubes under a moving nanoparticle. Part I: theoretical formulations Acta Mechanica, 216, 165-195.

[12] Fakhrabadi, M. M. S., Rastgoo, A. and Ahmadian, M. T. (2014). Dynamic analysis of carbon nanotubes under electrostatic actuation using modified couple stress theory. Acta Mechanica, 225, 1523-1535.

[13] Lu, P., Lee, H. P., Lu, P. C. and Zhang, P. Q. (2007). Application of nonlocal beam models for carbon nanotubes, International Journal of Solids and Structures, 44, 16, 5289–5300.

[14] Zhang, Y. G. Liu, G. and Han, X. (2005). Transverse vibration of double-walled carbon nanotubes under compressive axial load", Applied Physics Letter A, 340(1-4), 258–266.

[15] GhorbanpourArani, M.S. Zarei, M. Mohammadimehr, A. Arefmanesh, M.R. Mozdianfard. M. R. (2011).The thermal effect on buckling analysis of a DWCNT embedded on the Pasternak foundation", Physica E, 43, 1642–1648.

[16] He. J. H. (1999). Homotopy Perturbation Technique. Computer Methods in Applied Mechanics and Engineering, 178, 257-262.

[17] He, J. H. (2006). New Interpretation of Homotopy Perturbation Method. International Journal of Modern Physics B, 20, 2561-2568.

[18] He, J. H. (2000). A Coupling Method of Homotopy Technique and Perturbation Technique for Nonlinear Problems. International Journal of Non-Linear Mechanics, 35, 37-43.

[19] He, J. H. (2006). Some Asymptotic Methods for Strongly Nonlinear Equations. International Journal of Modern Physics B, 20, 1141-1199.

[20] He, J. H. (2000). New Perturbation Technique Which Is Also Valid for Large Parameters. Journal of Sound and Vibration, 229, 1257-1263.

[21] Rafei., M. and Ganji, D. D., Daniali, H. and Pashaei, H. (2007). The variational iteration method for nonlinear oscillators with discontinuities. J. Sound Vib, 305, 614–620.

[22] Ganji, S. S., Ganji, D. D., H. Babazadeh and Karimpour, S. (2008). Variational approach method for nonlinear oscillations of the motion of a rigid rod rocking back and cubic-quintic duffing oscillators. Prog. Electromagn. Res. M, 4, 23–32.

[23] Liao, S. J. (1992). The Proposed Homotopy Analysis Technique for the Solution of Nonlinear Problems,Ph. D. dissertation, Shanghai Jiao Tong University.

[24] Zhou, J. K. (1986). Differential Transformation and its Applications for Electrical Circuits. Huazhong University Press: Wuhan, China.

[25] Sobhan Mosayebidorcheh, O.D. Makinde , D.D. Ganji , and M. A. Chermahini. (2017). DTM-FDM hybrid approach to unsteady MHD Couette flow and heat transfer of dusty fluid with variable properties. Thermal Science and Engineering Progress, 2, 57-63.

[26] Mosayebidorcheh, S.Vatani, M. Ganji, D. D. and Mosayebidorcheh, T. (2014). Investigation of the viscoelastic flow and species diffusion in a porous channel with high permeability. Alexandria Engineering Journal, 53, 779–785.

[27] Mosayebidorcheh, S., Mosayebidorcheh, T. and Rashidi, M. M. (2014). Analytical solution of the steady state condensation film on the inclined rotating disk by a new hybrid method, Scientific Research and Essays, 9 (12), 557-565.

[28] Mosayebidorcheh, S., Rahimi-Gorji, M., Ganji, D. D. , Moayebidorcheh, T., Pourmehran, O. and Biglarian, M. (2017). Transient thermal behavior of radial fins of rectangular, triangular and hyperbolic profiles with temperature-dependent properties using DTM-FDM, Journal of Central South University, 24 (3), 675-682.

[29] Hatami, M., Mosayebidorcheh, S. Jing, D. (2017). Two-phase nanofluid condensation and heat transfer modeling using least square method (LSM) for industrial applications, Heat and Mass Transfer, 53 (6), 2061-2072.

[30] Fernandez, A. (2009). On some approximate methods for nonlinear models. Appl Math Comput, 215, 168-174.

[31] Sobamowo, M. G. (2016). Thermal analysis of longitudinal fin with temperature-dependent properties and internal heat generation using Galerkin's method of weighted residual. Applied Thermal Engineering, 99, 1316–1330.

[32] Eringen, A. C. (1983). On differential equations of nonlocal elasticity and solutions of screw dislocation and surface waves", Journal of Applied Physics, vol. 54(9), 4703–4710.

[33] Eringen, A. C. (1972). Linear theory of nonlocal elasticity and dispersion of plane waves", International Journal of Engineering Science, 10(5), 425–435.

[34] Eringen, A. C. and Edelen, D. G. B. (1972). On nonlocal elasticity", International Journal of Engineering Science, 10(3), 233–248.

[35] Sobamowo, M. G., Adeleye, O., Yinusa, A. A. (2017). Analysis of convective-radiative porous fin With temperature-dependent internal heat Generation and magnetic field using Homotopy Perturbation method, Journal of Computational and Applied Mechanics, Vol. 12., No. 2., pp. 127-145

[36] Sobamowo, M. G. Nonlinear vibration analysis of single-walled carbon nanotube conveying fluid with slip boundary conditions using variational iterative method, Journal of Applied and Computational Mechanics, 2016, 2(4), 208-221.

[37] Ali-Asgari, M., Mirdamadi, H. R. and Ghayour, M. (2013). Coupled effects of nano-size, stretching, and slip boundary conditions on nonlinear vibrations of nano-tube conveying fluid by the homotopy analysis method. Physica E, 52, 77–85

[38] Shokouhmand, H., Isfahani, A. H. M. and Shirani, E. (2010). Friction and heat transfer coefficient in micro and nano channels with porous media for wide range of Knudsen number", International Communication in Heat and Mass Transfer, 37, 890-894.